



Athanasiadou, G. E., Nix, A. R., & McGeehan, J. P. (1995). A new 3D indoor ray-tracing propagation model with particular reference to the prediction of power and delay spread. In International Symposium on Personal, Indoor and Mobile Radio Communications, 1995 (PIMRC'95). (Vol. 3, pp. 1161 - 1165). Institute of Electrical and Electronics Engineers (IEEE). 10.1109/PIMRC.1995.477329

Link to published version (if available):
[10.1109/PIMRC.1995.477329](https://doi.org/10.1109/PIMRC.1995.477329)

[Link to publication record in Explore Bristol Research](#)
PDF-document

University of Bristol - Explore Bristol Research

General rights

This document is made available in accordance with publisher policies. Please cite only the published version using the reference above. Full terms of use are available:
<http://www.bristol.ac.uk/pure/about/ebr-terms.html>

Take down policy

Explore Bristol Research is a digital archive and the intention is that deposited content should not be removed. However, if you believe that this version of the work breaches copyright law please contact open-access@bristol.ac.uk and include the following information in your message:

- Your contact details
- Bibliographic details for the item, including a URL
- An outline of the nature of the complaint

On receipt of your message the Open Access Team will immediately investigate your claim, make an initial judgement of the validity of the claim and, where appropriate, withdraw the item in question from public view.

A new 3D Indoor Ray - Tracing Propagation Model with particular reference to the prediction of power and delay spread

G.E. Athanasiadou, A.R. Nix and J.P. McGeehan

Centre for Communications Research, University of Bristol

Queen's Building, Bristol, UK

Fax: +44 (0)117 9255265, Tel: ++44 (0)117 9287740, E-mail: G.Athanasiadou@bristol.ac.uk

Abstract: In this paper a three dimensional 'image-based' ray tracing algorithm for indoor environments is presented. The model is capable of predicting wideband as well as narrowband propagation information for single floor scenarios. To show the practicality of such a model, the ray tracing engine has been used to investigate a typical indoor environment. The influence of internal objects such as windows, doors and partitions is considered. Since externally reflected and diffracted rays are supported, the impact of external building structures on the received power and rms delay spread is examined. The channel characteristics were also studied for different receiver antenna orientations.

I. INTRODUCTION

The need for more accurate propagation models will increase as indoor communication systems continue to evolve. Due to the site-specific nature of these environments, tools are required which take into account the location, the orientation and the electrical properties of individual walls and objects. At present, it is unlikely that existing empirical models will yield the accuracy and information required for future indoor planning. With this in mind, more attention is now being given to the development of indoor site specific propagation tools. Ray tracing produces deterministic channel models that operate by processing user-defined environments. It represents the high frequency limit of the exact solution for electromagnetic fields and can give good approximate solutions when it is impractical to obtain exact results.

In this paper an 'image-based' ray tracing model is presented that allows the rapid generation of complex channel impulse response characteristics for any given location of transmitter and receiver. In the algorithm, the image generation operates in two dimensions. However, for each two dimensional path, all the corresponding rays are then calculated in three dimensions including multiple floor-ceiling reflections. Factors such as polarisation and three dimensional antenna patterns are fully considered in the model for any antenna orientation. The simulation makes full use of reflection, transmission and diffraction and is capable of supporting indoor objects such as doors, windows and partitions. Moreover the model provides the ability to consider the influence of external building structures on the predicted indoor characteristics.

II. MODELLING APPROACH

THE IMAGE TECHNIQUE: Ray tracing represents electromagnetic waves as rays which are generated from a transmitter and launched in three dimensional space. There are many types of ray-tracing techniques reported in the literature [1-6]. In this model a technique based on the electromagnetic theory of images has been developed. Rather than using a 'ray launching' approach where rays are sent out at various angles and their paths traced until a power threshold is reached, the technique adopted here considers all walls and obstacles as potential reflectors and evaluates the location of their transmitter images [2]. This imaging technique works by conceptually generating an image table for each transmitter location. This process is implemented by considering all the various wall reflection, transmission and diffraction permutations that are possible in a given area. The image information is then stored in an array and used to compute the channel characteristics at each receiver location. To allow three dimensional paths to be found, a vertical ray trace is performed based on the results of the horizontal two dimensional image map. The situation for the simple line-of-sight case is illustrated in figure 1. The appropriate three dimensional rays can be calculated by considering the heights of the transmitter, receiver and ceiling.

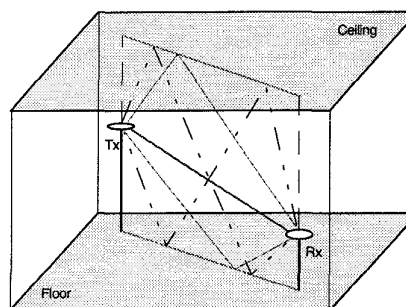


Fig. 1: 3D extension for the indoor environment

THE PROPAGATION MODEL: In a wireless communications system, the signal arriving at the receiver consists of several multipath components, each of which is the result of the interaction of the transmitted waves with the surrounding environment. The equation used to describe the mobile channel was first proposed by Turin [8] and takes the form of a bandlimited complex impulse response $h(t)$ given by:

$$h(t) = \sum_{n=1}^N A_n \delta(t - \tau_n) e^{-j\vartheta_n} \quad (1)$$

Here, the transmitted impulse is mathematically described by a Dirac function and the received signal $h(t)$ is formed from the vector addition of a number of time delayed rays, each represented by an attenuated and phase-shifted version of the original Dirac waveform. For each ray, the model computes the amplitude A_n , arrival time τ_n and arrival phase ϑ_n .

Reflected and transmitted rays are evaluated through the use of geometrical optics, while diffracted rays are calculated using the geometrical theory of diffraction [9]. According to the objects encountered by the i^{th} ray, its complex received field amplitude E_i (V/m) is given by:

$$E_i = E_0 f_{ti} f_{ri} \left\{ \prod_j R_j \prod_k T_k \prod_l A_l(s', s) D_l \right\} \frac{e^{-jkd}}{d} \quad (2)$$

where E_0 represents the transmitted field strength (V/m), f_{ti} and f_{ri} the transmitting and the receiving antenna field radiation patterns in the direction of the ray, R_j the reflection coefficient for the j^{th} reflector, T_k the wall transmission coefficient for the k^{th} transmission, D_l the diffraction coefficient for the l^{th} diffracting wedge and e^{-jkd} the propagation phase factor due to the path length d ($k = 2\pi/\lambda$). The diffraction coefficients are also multiplied by a spatial attenuation function $A_l(s', s)$ which finds the correct multiplicative diffraction coefficient given the d^{-1} dependence in the last term. All coefficients are functions of the angle of incidence and the object characteristics. In [2] a full explanation of the individual transmission, reflection and diffraction calculations can be found. The above approach is used to model the complex impulse response with no loss of phase information.

III. MODELLING ASSUMPTIONS

The model presented in this paper is capable of supporting three dimensional single floor scenarios. The field calculation is implemented using three dimensional vector analysis with each ray being considered separately. For each path found in the horizontal plane, the appropriate three dimensional rays are calculated by considering the multiple floor-ceiling reflections in a vertical plane (see figure 1). This vertical analysis continues until the rays fall below a certain pre-defined power threshold, however the process is suspended if part of the ray path travels outside the building. For such 'external' rays, only the direct ray is considered. Consequently, using this approach it is possible to model receiver positions outside of the building. In order to specify the limits of the indoor environment, external walls must be declared.

The model incorporates three dimensional antenna patterns for any orientation of the antenna. The code has

been developed to allow the user to steer the radiation pattern in any given direction. In the building database all the walls are assumed to be perpendicular to the floor but not necessarily to each other. In addition, the floor and ceiling are assumed to be both flat and parallel. As can be seen in figure 2, the program has been extended to support the modelling of partitions, i.e. walls with a fixed height less than the ceiling. Similarly, walls can also be modelled from the ceiling that do not necessarily reach the floor. However, for both cases the diffracted rays from their horizontal edges are currently not being considered. Objects such as tables and benches can also be modelled.

To make the algorithm as realistic as possible, walls with multiple windows and doors can be included in the data base. The model allows the width, height and position of each object to be defined. Hence, when a ray encounters such a wall, the algorithm selects the appropriate coefficients for the particular material and object concerned. Each wall is characterised by its permittivity, conductivity and thickness. Wall thickness is required in the calculation of reflected and transmitted field strengths [2]. The reflection and transmission coefficients are evaluated as a function of the incident angle for a range of different wall materials.

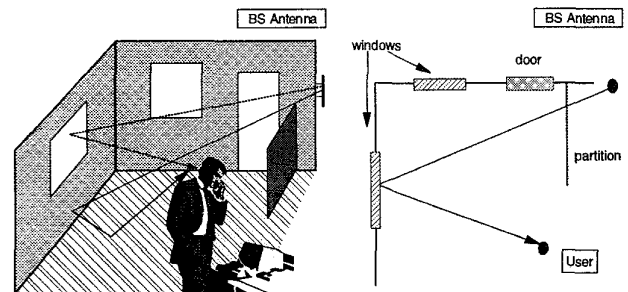


Fig. 2: Three Dimensional horizontal & vertical analysis

To maintain flexibility in the model, wall transmission and corner diffraction are fully supported even for onward propagating cases, i.e. each wall transmission or corner diffraction can undergo subsequent diffractions, reflections and transmissions. Although for microcellular studies wall transmission has often been ignored, for indoor studies transmission is an important propagation mechanism particularly for non-line-of-sight locations [7].

For each path, the maximum number of permitted transmissions, reflections and diffractions is defined by the user. The speed of the model is obviously a function of the number of objects in the building database and the number of reflections, transmissions and diffractions permitted in the ray engine. Due to the complex nature of the indoor environment, large amounts of memory can be required to store pre-processed 'image maps'. It is the generation of such image maps that greatly enhances the speed of the model.

IV. RESULTS

To show the practicality of this model the indoor environment illustrated in figure 3 has been examined. A 1W transmitter was placed at a height of 3.5m at location 'Tx' in figure 3. The transmitter and receiver were both modelled using standard dipole antennas. For the indoor locations the ceiling was set at a height of 4.5m. The map was created to contain a variety of rooms and corridors, each containing several windows, doors and partition walls. The electrical properties and characteristics of the doors and windows are those of wood and glass respectively. The floor, the ceiling and the various internal and external walls, are based on different types of stone and brick.

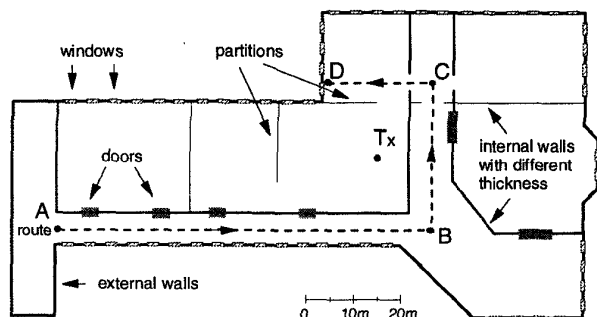


Fig. 3: Indoor environment

To illustrate how the average received power and time dispersion vary within the building, the route shown in figure 3 was defined to allow the user to 'walk' through a number of the indoor locations. The letters A-D at the top of the graphs refer to the route locations marked on figure 3. The receiving antenna height is 1.5m. The results were taken with 7 orders of reflection and 5 orders of wall transmission. Carrier frequencies of 1.8GHz, 5.2GHz and 17GHz were used in this study. The first frequency is representative of systems such as DCS1800 and DECT, the latter two frequencies represent the frequency bands allocated for the new ETSI European indoor radio LAN standard (HIPERLAN) [10].

Figure 4 shows the average received power for these three frequencies as the user moves slowly along the predefined route. Both transmitting and receiving dipoles are vertically polarised for this simulation. To obtain the average power at each point, the fast fading pattern was averaged over five wavelengths in two orthogonal directions. As expected, the path loss at higher frequencies is considerably larger. The rms delay spread, shown in figure 5, was calculated using a 30dB window relative to the profile peak. The channel dispersion is particularly high at the beginning of the route (A) and around locations (B) and (C). The initial results show rapid fluctuations in delay spread which seem to correspond with the locations of doors and the changing

number of walls between transmitter and receiver. At 17GHz the rms delay spread is lower than that predicted at 5.2GHz when the mobile moves closer to the transmitter.

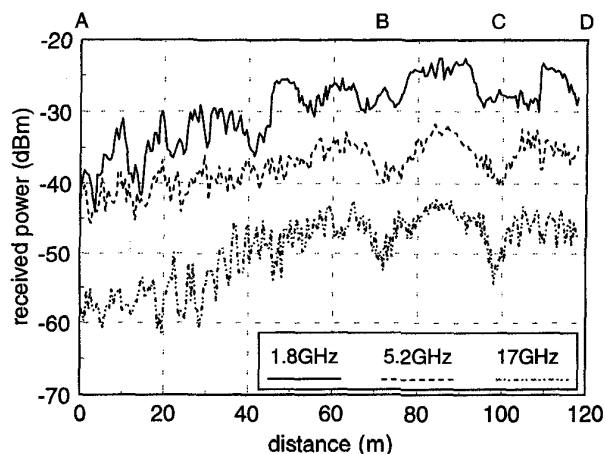


Fig. 4: Average received power along the route

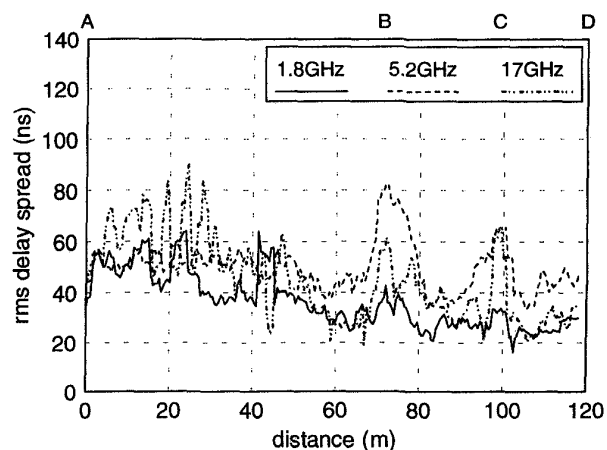


Fig. 5: Received rms delay spread along the route

Indoor propagation models tend to concentrate on analysing only the interior building structure. The following simulations were performed to determine the influence of neighbouring buildings in a dense urban environment. As shown in figure 6, eight neighbouring buildings were arranged around the indoor test environment. Since windows are accurately modelled, power can easily flow out of the building, interact with neighbouring objects, and then flow back into the indoor structure.

At each frequency the influence of the outside buildings had little effect on the average received signal power (2dB at most). As shown in figure 7, this was not the case for the rms delay spread. The results show a significant increase in received dispersion, the effects being particularly pronounced at higher frequencies and for positions away from the transmitter. As the carrier frequency increases, so does the

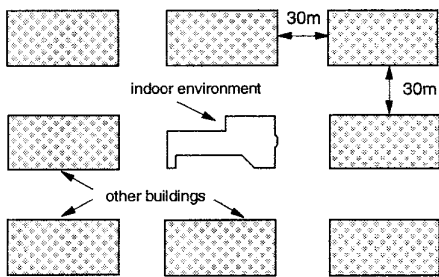


Fig. 6: Modelling the influence of external buildings

transmission loss through walls. Hence the internal rays at 17GHz become similar in magnitude to those transmitted through windows, resulting in a significant increase in the calculated rms delay spread. This is in contrast to 1.8GHz where the power flowing within the building tends to dominate over the rays reflected from external buildings.

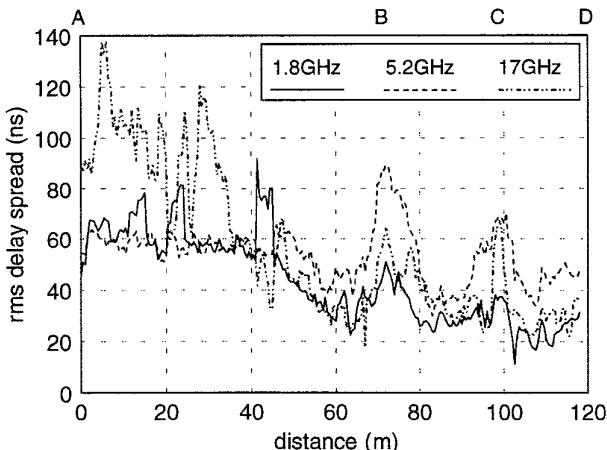


Fig. 7: Received rms delay spread (external objects)

With the transmitter still modelled as a vertically polarised dipole, the simulations were repeated for two horizontal dipoles, one vertical and one parallel to the route direction. The carrier frequency was set at 5.2GHz. Figures 8 and 9 show the average received power and the resulting cumulative distribution function for all three orientations. The power for the horizontal dipoles is on average 5dB lower than that of the vertical, although at some points it can be more than 10dB less. The dipole parallel to the route direction showed considerable variation in average power and at one location even exceeded the power received from the vertically polarised dipole. As shown in figure 10, both horizontal dipoles suffered large rms delay spread relative to the vertically oriented antenna. This is due to the fact that for these orientations most of the rays are of similar magnitude. Again the horizontal dipole parallel to the direction of travel had more variation and was very sensitive to the position of the surrounding objects.

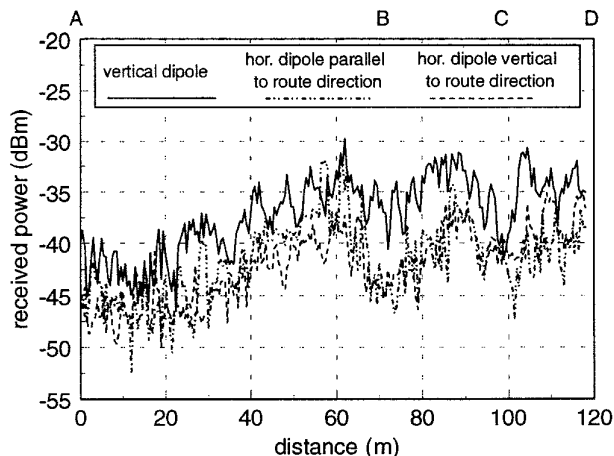


Fig. 8: Received power for horizontal and vertical dipoles

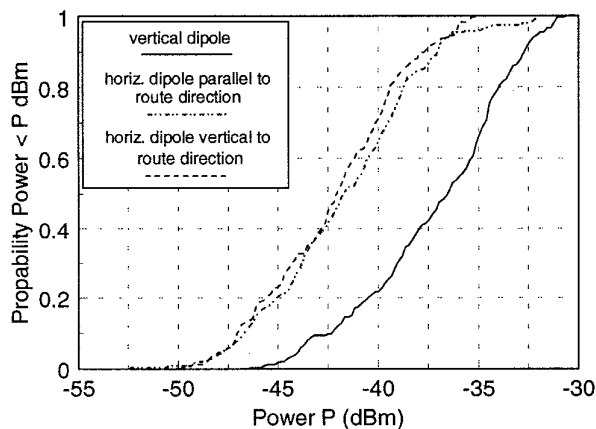


Fig. 9: CDF of the received power

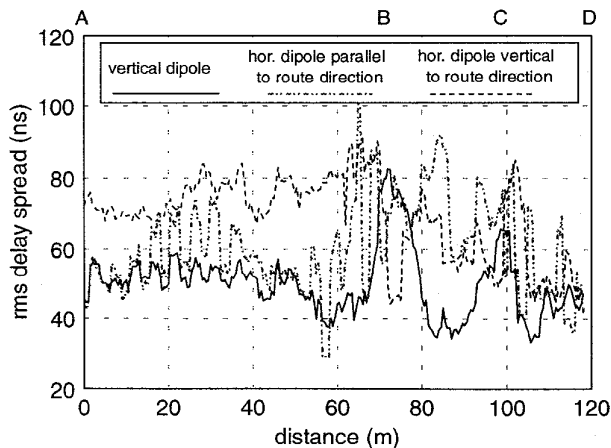


Fig. 10: RMS delay spread for different antenna orientations

Finally, figure 11 shows a graphical display of the average power and rms delay spread throughout the area. The results were taken for a carrier frequency of 5.2GHz, with the

receiver positioned at a height of 1 metre. Both the receiving and transmitting dipoles were vertically polarised. It is interesting to note the effects that the walls have on both the power and rms delay spread. By knowing the signal to noise ratio and the time dispersion that a system can tolerate, the quality of service can be predicted throughout the area. Similarly, the grid analysis can be used to optimise the location of the base station in a given environment.

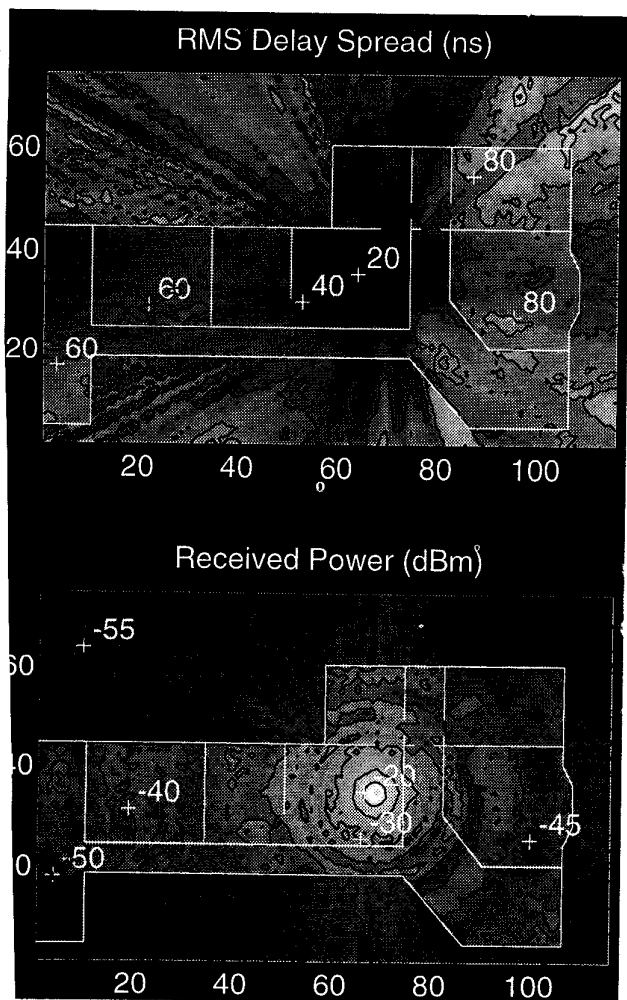


Fig. 11: Grid analysis of average received power and rms delay spread (axes in meters)

V. CONCLUSIONS

This paper has shown the viability of an 'image based' indoor propagation model for characterising the radio channel in both LOS and non-LOS locations. For the three frequencies that were considered, the average received power increased with increasing frequency, while the rms delay

spread was seen to be very sensitive both to the frequency and the surrounding objects. By exploiting the ability of the model to support different antenna orientations, three cases for the receiver antenna were studied. For these cases, when the transmitting and receiving antennas had different orientations, the received power was approximately 5dB lower on average, while the rms delay spread was seen to increase. Finally, the paper considered the influence of nearby external buildings and results show that they can have an important effect on the prediction of indoor rms delay spread.

ACKNOWLEDGEMENTS

G.E. Athanasiadou wishes to thank BNR Europe Ltd. for their financial support of this work. The authors would also like to acknowledge the support of their colleagues in the Centre for Communications Research and in particular Geoff Hilton and George Tsoulos.

REFERENCES

- [1] J.W. McKnown and R.L. Hamilton, "Ray-tracing as a design tool for radio networks", *IEEE Networks Mag.*, pp. 21-26, Nov. 1991.
- [2] M.C. Lawton, J.P. McGeehan, "The application of a deterministic ray launching algorithm for the prediction of radio channel characteristics in small-cell environments", *IEEE Trans. on Veh. Technol.*, vol. 43, no. 4, pp. 955-969, Nov. 1994.
- [3] S.Y. Seidel, T.S. Rappaport, "Site specific propagation prediction for wireless in-building personal communication system design", *IEEE Trans. Veh. Technol.*, vol. 43, no 4, pp. 879-891, November 1994.
- [4] W. Honcharenko, H.L. Bertoni, J.L. Dailing, J. Qian, H.D. Yee, "Mechanisms governing UHF propagation on single floors in modern office buildings", *IEEE Trans. Veh. Technol.*, vol. 41, no 4, pp. 496-504, November 1992.
- [5] K.J. Gladstone and J.P. McGeehan, "Computer simulation of multipath fading in the land mobile radio environment", *IEE Proc.*, vol. 27, Pt.G., pp.323-330, no. 6, Dec.1980.
- [6] R.A. Valenzuela, "A ray tracing approach to predicting indoor wireless transmission", *43rd IEEE VTC*, New Jersey, May 1993.
- [7] G.E. Athanasiadou, A.R. Nix, J.P. McGeehan, "An efficient 'image-based' propagation model for LOS and non-LOS applications", *IEE Colloquium on propagation in buildings, 1995/134*, June 1995.
- [8] G.L. Turin et.al. "A statistical model for urban multipath propagation", *IEEE Trans. Veh. Technol.*, vol. VT-21, pp. 1-9, Feb. 1972.
- [9] J.B. Keller, "Geometrical Theory of Diffraction", *J. Opt. Soc. Amer.*, vol. 52, pp. 116-130, February 1962
- [10] A. Nix, M. Li, J. Marvill, T. Wilkinson, I. Johnson, S. Barton, "Modulation and Equalisation Considerations for High Performance Radio LANs (HIPERLAN)", *IEEE PIMRC*, pp 964 - 968, Sept. 1994.